JOURNAL OF VIROLOGY, May 2007, p. 4633–4644 Vol. 81, No. 9
0022-538X/07/$08.00+0 doi:10.1128/JVI.02267-06

Nodavirus RNA Replication Protein A Induces Membrane Association of Genomic RNA[▽]

Priscilla M. Van Wynsberghe,[1] Hau-Ren Chen,[1]† and Paul Ahlquist[1,2]*

Institute for Molecular Virology[1] and Howard Hughes Medical Institute,[2] University of Wisconsin—Madison, Madison, Wisconsin 53706

Received 16 October 2006/Accepted 7 February 2007

Positive-strand RNA virus genome replication occurs in membrane-associated RNA replication complexes, whose assembly remains poorly understood. Here we show that prior to RNA replication, the multifunctional, transmembrane RNA replication protein A of the nodavirus flock house virus (FHV) recruits FHV genomic RNA1 to a membrane-associated state in both *Drosophila melanogaster* and *Saccharomyces cerevisiae* cells. Protein A has mitochondrial membrane-targeting, self-interaction, RNA-dependent RNA polymerase (RdRp), and RNA capping domains. In the absence of RdRp activity due to an active site mutation (A_{D692E}), protein A stimulated RNA1 accumulation by increasing RNA1 stability. Protein A_{D692E} stimulated RNA1 accumulation in wild-type cells and in *xrn1*$^-$ yeast defective in decapped RNA decay, showing that increased RNA1 stability was not due to protein A-mediated RNA1 recapping. Increased RNA1 stability was closely linked with protein A-induced membrane association of the stabilized RNA and was highly selective for RNA1. Substantial N- and C-proximal regions of protein A were dispensable for these activities. However, increased RNA1 accumulation was eliminated by deleting protein A amino acids (aa) 1 to 370 but was restored completely by adding back the transmembrane domain (aa 1 to 35) and partially by adding back peripheral membrane association sequences in aa 36 to 370. Moreover, although RNA polymerase activity was not required, even small deletions in or around the RdRp domain abolished increased RNA1 accumulation. These and other results show that prior to negative-strand RNA synthesis, multiple domains of mitochondrially targeted protein A cooperate to selectively recruit FHV genomic RNA to membranes where RNA replication complexes form.

All positive-strand RNA viruses replicate in association with intracellular membranes. The particular membrane(s) used during RNA replication varies, with many positive-strand RNA viruses replicating in association with the endoplasmic reticulum, while others use lysosomal, mitochondrial, peroxisomal, or other membranes (16, 17, 26, 28, 36, 42, 43, 45, 55, 56, 60). Some viral RNA replication proteins carry membrane-targeting signals and interact with other viral proteins to localize these to the sites of RNA replication complex formation (18, 56, 58, 62). In a few cases, interactions contributing to recruitment of viral RNA replication templates have also been identified. Brome mosaic virus (BMV) helicase-like protein 1a, e.g., induces formation of spherular endoplasmic reticulum membrane invaginations and selectively recruits BMV 2a polymerase and BMV genomic RNAs to these structures to form RNA replication complexes (1, 11, 12, 32, 62, 66). Similarly, tomato bushy stunt virus replication protein p33 binds defective interfering RNA (DI-RNA) in vitro, and the related cucumber necrosis virus p33 protein recruits such RNAs to replication complex sites in vivo (47, 48, 51, 54).

Flock house virus (FHV) is the best-studied member of the alphanodaviruses in the *Nodaviridae* family. The bipartite FHV genome consists of RNA1 (3.1 kb) and RNA2 (1.4 kb), which encode protein A, a multifunctional RNA replication factor, and the capsid precursor, respectively (7, 13, 21–23). Both genomic RNAs are capped, nonpolyadenylated, and copackaged into a nonenveloped icosahedral capsid with T=3 symmetry (61, 63). RNA1 also encodes a subgenomic RNA, RNA3, which translates B2, a 12-kDa RNA silencing inhibitor (20, 22, 27, 38).

FHV protein A (112 kDa) contains an RNA-dependent RNA polymerase (RdRp) domain, self-interaction domains, a putative RNA capping domain, and an N-terminal mitochondrial targeting and transmembrane domain that mediates protein A localization and insertion into the outer mitochondrial membrane, where FHV RNA replication occurs in association with spherular membrane invaginations strikingly similar to those of BMV (15, 33, 35, 44, 45, 62). Based on amino acid similarity within eight distinct RdRp motifs, protein A belongs to the positive-strand RNA RdRp supergroup I (34, 35). The sixth RdRp motif contains a GDD motif that is conserved among RdRps of all positive-strand RNA viruses and is required for metal ion coordination in the polymerase active site (4, 9, 34, 35). Mutation of the GDD motif inhibits polymerase activity in many viruses, such as hepatitis C virus, poliovirus, and FHV (9, 31).

FHV was originally isolated from the insect *Costelytra zealandica* and also productively infects *Drosophila melanogaster* cells. In addition, FHV can replicate in animal, plant, *Caenorhabditis elegans*, and *Saccharomyces cerevisiae* cells if RNA templates are provided by transfection or DNA expression (6, 21, 40, 52, 63, 64). Like *Drosophila*, the budding yeast *Saccharomyces cerevisiae* supports autonomous replication of RNA1, infectious virion production, RNA2 inhibition of RNA3 replication, distinct mitochondrial membrane alterations, and other features of natural FHV infection (39, 45, 46, 52, 53).

* Corresponding author. Mailing address: Institute for Molecular Virology, University of Wisconsin—Madison, 1525 Linden Dr., Madison, WI 53706-1596. Phone: (608) 263-5916. Fax: (608) 265-9214. E-mail: ahlquist@facstaff.wisc.edu.

† Present address: Institute of Molecular Biology, National Chung Cheng University, Chia-Yi 621, Taiwan, Republic of China.

▽ Published ahead of print on 14 February 2007.

Here we show that FHV protein A selectively induces RNA1 association with membranes in the absence of negative-strand RNA1 synthesis. Simultaneously, protein A increases in vivo FHV RNA1 stability and accumulation. The protein A membrane association domain and regions surrounding and including the RdRp domain are required for these activities, while significant regions of the N and C termini and some protein-protein interaction domains are dispensable. Overall, the results imply that in a distinct step prior to negative-strand RNA synthesis, the mitochondrially localized transmembrane protein A recruits FHV RNA1 to the membrane-associated sites of RNA replication complex formation.

MATERIALS AND METHODS

Plasmids. Standard molecular cloning techniques were used throughout (5, 59). All products generated by PCR were verified by sequencing. Detailed methods and primer sequences will be provided upon request. Numbering of FHV RNA1 sequences is based on GenBank accession number NC_004146. FHV RNA expression plasmids for $RNA1_{fs}$ ($pF1_{fs}$) and protein A_{wt} (pFA) have been described previously (39, 44, 46, 52, 53). $pF1_{fs}$ and pF1 are *HIS3*-selectable yeast centromeric plasmids that contain full-length RNA1 flanked by the *GAL1* promoter and the hepatitis delta virus ribozyme (pF1 was provided courtesy of D. Miller). A 4-nucleotide (nt) insertion at nt 373 in $pF1_{fs}$ causes a frameshift in the protein A open reading frame (ORF). pFA is a *LEU2*-selectable yeast centromeric plasmid that contains protein A mRNA flanked by the *GAL1* promoter and leader sequence at the 5′ end and a 3′ *CYC1* polyadenylation signal.

(i) pFA_{D692E}. pFA was amplified with two sets of primers that yielded overlapping PCR products containing a T-to-A mutation at nt 2115. PCR products were mixed, amplified with bordering primers, digested with BlpI and RsrII, and ligated into common sites in pFA.

(ii) pFA-YFP and pFA_{D692E}-YFP. The C-terminal coding region of pFA and the yellow fluorescent protein (YFP) ORF of a protein A-YFP fusion-expressing plasmid (courtesy of B. Dye) were amplified by PCR with overlapping primers at the protein A mRNA-YFP mRNA junction. PCR products were mixed, amplified with bordering primers, digested with HindIII and BlpI, and ligated into common sites in pFA and pFA_{D692E} to make pFA-YFP and pFA_{D692E}-YFP, respectively. Both plasmids contain a stop codon after the protein A ORF.

(iii) pGlobin. pGlobin, previously described as GAL-IRA or pMS99 (66), contains the β-globin ORF flanked by the *GAL1* promoter and leader at the 5′ end and the alcohol dehydrogenase 1 (*ADH1*) 3′-untranslated region (UTR).

(iv) pYFP. pYFP contains the YFP ORF flanked by the *GAL1* promoter and the *ADH1* 3′UTR. The *GAL1* promoter region and the YFP ORF of pA-YFP were amplified with primers that overlap at the *GAL1* promoter-YFP mRNA junction. PCR products were mixed, amplified with bordering primers, digested with AgeI and XbaI, and ligated into common sites in pGlobin.

(v) YFP probe template. The YFP ORF was amplified and ligated into pGEM-T with a Promega pGEM-T Easy Vector System I kit (Madison, WI). The YFP ORF was cut out of the pGEM-T vector with SacII and XhoI and ligated into common sites in pBluescript II KS(+) (Stratagene, La Jolla, CA).

(vi) Protein A deletions. A two-step PCR process was used to make all protein A deletions. First, two protein A sequences that flanked the deletion region were amplified. The PCR products were then combined, amplified with bordering primers, digested, and ligated into common sites in PFA_{D692E} or pFA_{D692E}-YFP.

(vii) *Drosophila* expression plasmids. All FHV expression plasmids were derivatives of $pIE1^{hr}$/PA, which contains the baculovirus immediate-early 1 (IE1) promoter, the baculovirus transactivating *hr*5 enhancer, and a polyadenylation signal (10). pIE1-$F1_{fs}$ was made by amplifying RNA1 from pF1 and ligating the PstI- and SalI-digested product into common sites in $pIE1^{hr}$/PA. pIE1-FA was made by amplifying the protein A ORF from pFA and ligating the HindIII- and SalI-digested product into common sites in $pIE1^{hr}$/PA. pIE1-FA_{D692E} was made by ligating the NcoI-digested protein A_{D692E} insert into common sites in pIE1-FA.

Cells. The haploid yeast strains YPH500 (*MATα ura3-52 lys2-801 ade2-101 trp1-Δ63 his3-Δ200 leu2-Δ1*) and YPH500 *xrn1*$^-$ (*MATα ura3-52 lys2-801 ade2-101 trp1-Δ63 his3-Δ200 leu2-Δ1 xrn1Δ Bgl::URA3*) were transformed by using an E-Z transformation kit (Zymo Research, Orange, CA) (44). Yeast cells were grown in 2% glucose selective medium for 2 days at 30°C. DNA-directed RNA expression was induced by growth of yeast in 2% galactose selective medium for 16 to 20 h, to mid-log phase (optical density at 600 nm, 0.75 to 1.0). *Drosophila melanogaster* S2 cells were grown at 28°C in *Drosophila* serum-free medium (SFM) supplemented with 17 mM L-glutamine (Gibco, Carlsbad, CA). For transfections, 25 μg of plasmid DNA in 500 μl SFM was mixed with an equal volume of SFM containing 160 μl of DOTAP-DOPE {*N*-[1-(2,3-dioleoyloxy)propyl]-*N*,*N*,*N*-trimethylammonium chloride salt and L-(phosphatidylethanolamine, dioleoyl)} liposomes for 30 min at room temperature (Sigma, St. Louis, MO). The DNA and DOTAP-DOPE mixture was then added to previously plated S2 cells (1×10^7 to 3×10^7 cells/T75 flask) in 3 ml of SFM.

Antibodies. A rabbit polyclonal antibody against protein A was described previously (45). Mouse monoclonal antibodies against yeast 3-phosphoglycerate kinase (PGK) and mitochondrial porin were purchased from Molecular Probes (Eugene, OR). Rabbit polyclonal antibody against mitochondrial porin/voltage-dependent anion channel was obtained from Affinity Bioreagents (Golden, CO). Rabbit polyclonal antibody against actin was obtained from Santa Cruz Biotechnology, Inc. (Santa Cruz, CA). Alkaline phosphate-conjugated secondary antibodies were purchased from Bio-Rad (Hercules, CA).

RNA extraction and Northern blot analysis. Total RNA from yeast or *D. melanogaster* cells was isolated and prepared by the hot phenol method (39). Northern blotting was performed as previously described, except that 2 or 4 μg RNA was separated in 1% (wt/vol) agarose-MOPS (morpholinepropanesulfonic acid)-formaldehyde gels (39). Probes against globin and positive- and negative-strand RNA1 and RNA3 have been described (52, 66). Probes against 18S rRNA were derived from pTRI RNA 18S templates (Ambion, Austin, TX). Probe templates against the DEAD box protein 2 (*DBP2*), pyruvate kinase 1 (*PYK1*), and alcohol dehydrogenase 1 (*ADH1*) genes were made by amplifying 400 to 500 nt of their respective cDNAs (courtesy of D. Kushner) with an Ambion Lig'n Scribe kit (Austin, TX). The actin mRNA probe targeted a 315-nt fragment of *actin* mRNA expressed from pBluescript II KS(+) (Stratagene, La Jolla, CA). Probes were synthesized using either a Strip-EZ RNA kit from Ambion (Austin, TX) or an Epicenter Riboscribe probe synthesis kit (Madison, WI) with the appropriate enzyme, i.e., T7, T3, or SP6 polymerase. Northern blots were imaged on a Typhoon 9200 instrument (Amersham Biosciences, Piscataway, NJ). Band intensities were analyzed with ImageQuant software (Molecular Dynamics, Piscataway, NJ).

Protein extraction, Western blotting, and total protein analysis. For Fig. 1, 2, 8, and 9, total protein was extracted from yeast as described previously (44). For Fig. 6B, to prevent the loss of material, yeast or *Drosophila* cells were resuspended in a 1% solution of β-mercaptoethanol and sodium dodecyl sulfate (SDS), boiled, vortexed, and supplemented with cracking buffer (10 ml total, containing 0.8 g SDS, 1.4 g Ficoll, 2 ml β-mercaptoethanol, 5 ml of 0.5 M Tris-HCl, pH 6.8, and bromphenol blue). Cell lysates were separated in 10% SDS-polyacrylamide gels and immunoblotted, and chemiluminescence was detected with a Boehringer Mannheim Lumi-Imager as described previously (45). The total protein concentration was determined with a reducing agent-compatible BCA protein assay kit (Pierce, Rockford, IL).

RNA half-life. Yeast cells were grown and induced as described above and then resuspended at an optical density at 600 nm of 1.0 in 2% dextrose selective medium. Aliquots (1 ml) were taken in duplicate 0, 5, 15, 30, 60, and 120 min after resuspension (66) and frozen on dry ice before RNA and protein extraction as described above. Equal RNA concentrations and protein lysate volumes were analyzed by Northern and Western blotting, respectively. *Drosophila* cells were transfected and grown as described above. Two days after transfection, cell suspensions were treated with actinomycin D at 20 μg/ml and incubated on a rotator at room temperature. Aliquots (100 μl) were taken 0, 15, 30, 60, 90, 120, 150, 180, 210, and 240 min after treatment and frozen on dry ice before RNA extraction and subsequent analysis by Northern blotting as described above.

Membrane flotation. Yeast cells were prepared for membrane flotation, spheroplast formation, and lysis by Dounce homogenization as described previously (44). *Drosophila* cells were collected 2 days after transfection and incubated in flotation buffer [50 mM piperazine-*N*,*N*′-bis(2-ethanesulfonic acid) (PIPES), pH 7.4, 50 mM KCl, 5 mM EDTA, 2 mM $MgCl_2$, 1 mM dithiothreitol, 4 mM ribonucleoside vanadyl complex (New England Biolabs, Beverly, MA), and protease inhibitor cocktail (Sigma, St. Louis, MO)] for 10 min at 4°C before lysis by 100 strokes with a Dounce homogenizer. Cell debris, unlysed cells, and nuclei were extracted from either yeast or *Drosophila* cells by centrifugation at $500 \times g$ for 5 min. Cell lysates were mixed with Nycodenz to a final concentration of 37.5%, loaded under a 5 to 35% Nycodenz discontinuous gradient, and centrifuged at $100{,}000 \times g$ for 4 to 5 h in a Beckman TLS-55 swing-bucket rotor. Six equal fractions were collected from each gradient. RNAs were isolated from half of each fraction by hot phenol RNA extraction as described above. Equal amounts of RNA, based on the bottom fraction's concentration, were analyzed by Northern blotting or real-time reverse transcription-PCR (RT-PCR), as de-

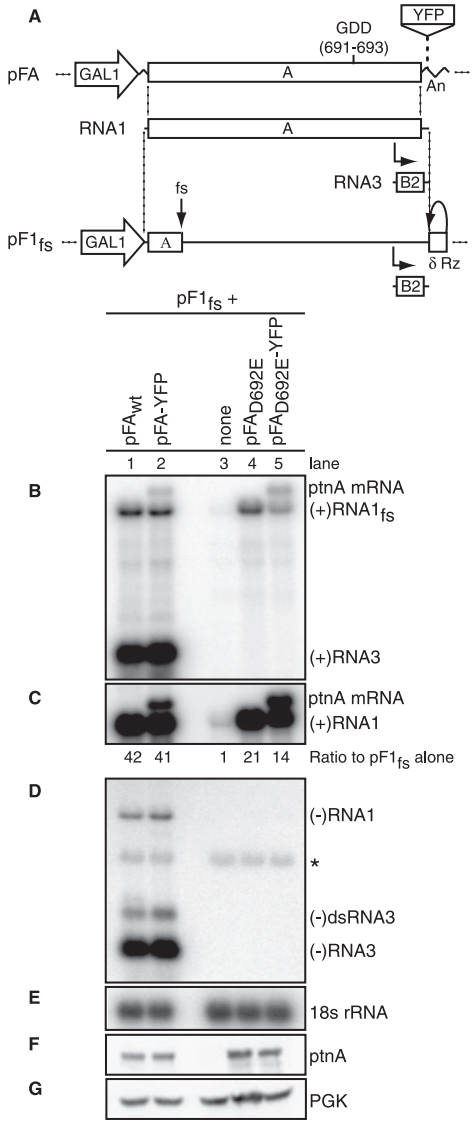

FIG. 1. Protein A stimulates $RNA1_{fs}$ accumulation. (A) Schematic of plasmid-directed $RNA1_{fs}$ and protein A expression in yeast. $pF1_{fs}$ expresses $RNA1_{fs}$ from a *GAL1* promoter, with a hepatitis delta virus ribozyme-mediated authentic 3′ end (δ Rz). Insertion of a 4-nt sequence causes a frameshift (fs) in RNA1 that prevents full-length protein A production. pFA encodes protein A mRNA flanked by a *GAL1* leader sequence and a *CYC1* polyadenylation signal (An). The protein A GDD polymerase motif occurs at aa 691 to 693. Insertion of YFP mRNA downstream of and separate from the protein A mRNA increases the size of protein A mRNA. (B to G) Representative data from seven independent experiments are shown. Total RNA and total protein were isolated from yeast cells transformed with $pF1_{fs}$ alone or together with pFA, pFA-YFP, pFA_{D692E}, or pFA_{D692E}-YFP. Total RNA (2 μg) was analyzed by Northern blotting with ^{32}P-labeled cRNA probes for positive-strand $RNA1_{fs}$ and RNA3 (B and C), negative-strand RNA1 and RNA3 (D), and 18S rRNA (E). The blot in panel C was exposed 100 times longer than that in panel B to allow for visualization of positive-strand $RNA1_{fs}$ in lane 3. Panels C and D had the same exposure time. The asterisk represents a background band (D). Total protein was analyzed by Western blotting with antibodies against protein A (F) and the cytoplasmic yeast protein PGK (G).

scribed above and below, respectively. Half of each fraction was mixed with 3× protein loading buffer for protein analysis by Western blotting.

RNA analysis by real-time RT-PCR. RNAs from membrane flotation assays in *Drosophila* cells or from total RNA assays in yeast and *Drosophila* cells were treated with DNase by use of an Ambion Turbo DNA-free kit (Austin, TX). Five nanograms of RNA (5 ng), based on the bottom fraction concentration, or total RNA (75 ng) was analyzed by real-time RT-PCR for positive-strand $RNA1_{fs}$ or actin mRNA with a Taqman one-step RT-PCR master mix reagent kit (Applied Biosystems, Foster City, CA) in an Applied Biosystems 7900 machine at a 9600 emulation setting (Foster City, CA). The conditions were as follows: 1× master mix without uracil-*N*-glycosylase (AmpliTaq gold enzyme, deoxynucleoside triphosphates, ROX, and buffer), 0.25 units/μl Multiscribe and RNase inhibitor mix, a 700 μM concentration of each primer, 350 μM probe, and water to 10 μl. The PCR conditions were as follows: 48°C for 30 min, 95°C for 10 min, and 40 cycles of 95°C for 15 s and 60°C for 1 min. Primer and probe pairs were designed with the Primer Express program (Applied Biosystems, Foster City, CA), and their sequences are available upon request. The *Drosophila actin* probe was described previously (50). The RNA1 forward primer, reverse primer, and probe initiated at nt 23, 153, and 110, respectively. The *Drosophila actin* forward and reverse primers initiated at nt 507 and 748, respectively.

Cell fractionation. Spheroplasted yeast cells were divided into two fractions and lysed by vigorous pipetting in lysis buffer (50 mM Tris-Cl, pH 7.4, 10 mM ribonucleoside vanadyl complex [New England Biolabs, Beverly, MA]). Centrifugation of half of each sample at 20,000 × *g* for 5 min separated the membrane-enriched pellet (P) from the supernatant (S) fraction. RNAs were extracted from the pellet, supernatant, and unspun (total [T]) fractions by successive treatments with acidic phenol, phenol-chloroform, and 100% ethanol with sodium acetate. Equal RNA amounts, based on the total RNA concentration, were analyzed by Northern blotting.

RESULTS

Protein A stimulates $RNA1_{fs}$ accumulation. To study the effects of protein A on RNA1 prior to virus-induced RNA synthesis, a previously documented, polymerase-inactivating D-to-E mutation was made at the first aspartate (amino acid [aa] 692) in the conserved GDD motif of the polymerase domain of protein A (9, 31). The resulting mutant and wild-type (wt) protein A were expressed from plasmids pFA_{D692E} and pFA, respectively (Fig. 1A). These plasmids contain the protein A ORF but lack the 5′- and 3′-noncoding regions of RNA1, including *cis*-acting signals essential for RNA1 replication (39). Accordingly, the resulting transcripts of pFA and pFA_{D692E} did not serve as replication templates for protein A. For a replication template, we used the previously characterized RNA1 derivative $RNA1_{fs}$, which bears the full-length sequence of RNA1 together with a frameshift that blocks protein A expression (Fig. 1A) (39). This *trans*-replication system separates the *cis*- and *trans*-acting RNA replication functions of RNA1 onto separate plasmids for independent manipulation (39).

In yeast cells, viral RNAs were under the control of the *GAL1* promoter. *cis* cleavage by a flanking hepatitis delta virus antigenomic ribozyme produced a wt 3′ end on $RNA1_{fs}$, while the addition of a *CYC1* poly(A) tail protected protein A mRNA (Fig. 1A). Total RNA was collected, and 2 μg of total RNA was analyzed by Northern blotting. All experiments were repeated at least three times, and representative results are shown. Expression of $pF1_{fs}$ alone in yeast yielded very low levels of positive-strand $RNA1_{fs}$ because its only source was cellular transcription from the *GAL1* promoter (Fig. 1B and C, lanes 3). However, when $pF1_{fs}$ and pFA were coexpressed, *trans*-replication of $RNA1_{fs}$ occurred, as seen by the presence of negative-strand $RNA1_{fs}$ and positive- and negative-strand RNA3 (Fig. 1B to D, lanes 1). As expected, positive-strand

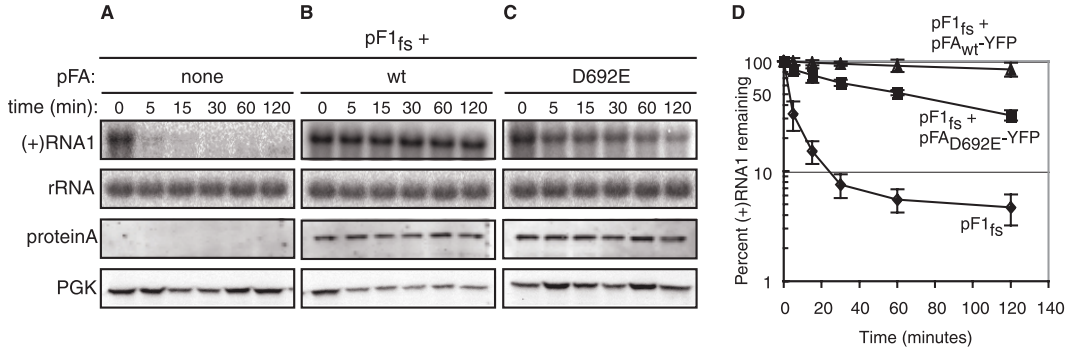

FIG. 2. Protein A stimulates $RNA1_{fs}$ stabilization. Yeast cells transformed with $pF1_{fs}$ alone (A) or together with pFA_{wt}-YFP (B) or pFA_{D692E}-YFP (C) were grown in selective galactose medium to mid-log phase and then switched to selective glucose medium. Total RNAs and total proteins were isolated from equal volumes of yeast cells collected 0 to 2 hours after the switch to selective glucose medium and were analyzed by Northern and Western blotting as described in the legend to Fig. 1. RNA levels, determined from five independent experiments, were graphed as the percentage of positive-strand $RNA1_{fs}$ remaining compared to that at time zero (D).

$RNA1_{fs}$ and RNA3 levels were about 25-fold higher than negative-strand RNA1 and RNA3 levels. (Fig. 1C and D had the same exposure time, which was 100 times longer than that for Fig. 1B, and the positive- and negative-strand RNA1 and RNA3 probes had comparable relative radioactivities).

To independently follow the effects of protein A on its mRNA and $RNA1_{fs}$, the YFP ORF was inserted into pFA downstream of and separated from the protein A ORF (pFA-YFP) (Fig. 1A). This allowed wt protein A expression but increased the size of protein A mRNA by ~700 nucleotides. Expression of pFA-YFP and $pF1_{fs}$ produced a second band above the positive-strand $RNA1_{fs}$ band that corresponded to the YFP ORF-augmented protein A mRNA (Fig. 1B and C, lanes 2). Protein A levels were equivalent in the presence of either pFA or pFA-YFP (Fig. 1F).

As expected, coexpression of $pF1_{fs}$ and pFA_{D692E} produced neither negative-strand $RNA1_{fs}$ nor positive- or negative-strand RNA3 (Fig. 1B to D, lanes 4). However, even in the absence of protein A polymerase activity, pFA_{D692E} markedly stimulated positive-strand $RNA1_{fs}$ accumulation (Fig. 1B and C, lanes 4). To isolate protein A's effects on its own mRNA from those on $RNA1_{fs}$ prior to RNA synthesis, pFA_{D692E}-YFP was used. Expression of pFA_{D692E}-YFP and $pF1_{fs}$ caused a 14-fold increase in $RNA1_{fs}$ accumulation over that from $pF1_{fs}$ alone (Fig. 1B and C, lanes 5). The sum of the protein A mRNA and $RNA1_{fs}$ bands in Fig. 1B, lanes 2 and 5, was equivalent to the positive-strand RNA1 band intensities in Fig. 1B, lanes 1 and 4, respectively, which contained both protein A mRNA and $RNA1_{fs}$. Similar protein A levels were expressed from pFA_{D692E} and pFA_{D692E}-YFP (Fig. 1F). Protein A did not affect the 18S rRNA or PGK protein level (Fig. 1E and G).

Protein A stimulates $RNA1_{fs}$ stabilization. Protein A_{D692E}-stimulated RNA1 accumulation in the absence of protein A polymerase activity might result from stimulating plasmid-directed RNA1 transcription or inhibiting RNA1 degradation. To investigate the first possibility, run-on transcription assays were performed (32). Protein A_{D692E} did not increase the DNA-dependent transcription of RNA1, other cellular mRNAs such as actin, or other nonyeast genes, such as globin or YFP, introduced via plasmid transformation (data not shown).

To analyze protein A effects on FHV RNA1 stability by half-life analysis, we took advantage of the tightly regulated galactose-inducible, glucose-repressible *GAL1* promoter. Yeast cells transformed with the appropriate viral plasmids were grown in selective galactose medium overnight to induce $RNA1_{fs}$ and protein A mRNA transcription. Viral RNA transcription via the *GAL1* promoter was shut off by switching yeast cells grown to mid-log phase to selective glucose medium. Yeast cells were collected at six time points over a 2-hour period after this glucose-induced shutoff, and equal amounts of total RNA were isolated and analyzed by Northern blotting. When expressed alone, $RNA1_{fs}$ rapidly degraded, with a half-life of less than 5 minutes, while 18S rRNA and PGK protein levels remained constant (Fig. 2A). The entire blot intensity for $pF1_{fs}$ alone (Fig. 2A, top panel) was substantially enhanced relative to that for Fig. 2B and C to allow for visualization of the time zero $RNA1_{fs}$ band. The actual relative band intensities of $RNA1_{fs}$ alone compared to $RNA1_{fs}$ with protein A_{D692E}-YFP under these conditions are shown in Fig. 1B, lanes 3 and 5, respectively. Time course analysis (Fig. 2D) was used to calculate the $RNA1_{fs}$ half-life. Dissecting the $pF1_{fs}$ curve revealed two pools of $RNA1_{fs}$. One pool, containing >90% of the $RNA1_{fs}$ transcripts, degraded rapidly, with a half-life of about 4 minutes. In contrast, about 5% of the $RNA1_{fs}$ transcripts persisted with a much longer half-life throughout the time course studied, suggesting a second, minor pool, such as nuclear transcripts.

Coexpressing wt protein A from pFA_{wt}-YFP and $pF1_{fs}$ maintained a nearly constant level of $RNA1_{fs}$ per cell after glucose-induced shutoff (Fig. 2B), representing the steady-state level of $RNA1_{fs}$ maintained by RNA replication in the rapidly dividing yeast cells (Fig. 1B and D). In the absence of protein A polymerase activity, protein A_{D692E}-YFP dramatically enhanced $RNA1_{fs}$ stability to a half-life of ~66 min (Fig. 2C and D). Since the PGK protein is an abundantly expressed cytoplasmic protein in yeast and the PGK1 mRNA is very stable (half-life is 45 min), the PGK protein was used as a control (Fig. 2) (29). Despite occasional fluctuations in individual measurements, 18S rRNA, PGK protein, and protein A (where expressed) levels were constant, on average, at all time points (Fig. 2A to C).

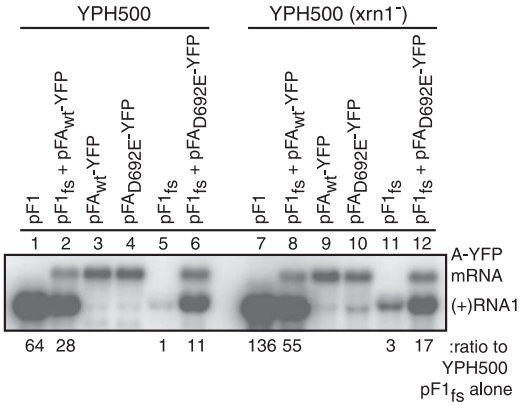

FIG. 3. Protein A increases $RNA1_{fs}$ accumulation in yeast defective in the mRNA decay pathway (*xrn1*$^-$). YPH500 cells (wt or *xrn1*$^-$) were transformed with pF1, $pF1_{fs}$ plus pFA_{wt}-YFP, pFA_{wt}-YFP, pFA_{D692E}-YFP, $pF1_{fs}$, or $pF1_{fs}$ plus pFA_{D692E}-YFP. Total RNA was isolated and analyzed by Northern blotting as described in the legend to Fig. 1. Representative Northern blots from four independent experiments are shown.

Increased $RNA1_{fs}$ accumulation is not due to protein A-mediated RNA recapping. RNA1 is sufficient for viral replication, and protein A contains a proposed guanylylation site that is suggestive of guanylyltransferase activity (33). Consequently, protein A likely adds the 5′ 7-methylguanosine caps found on FHV genomic RNAs (33). In yeast, the major mechanism of mRNA decay occurs by decapping followed by Xrn1p-mediated 5′-to-3′ degradation (37, 65, 67). Because selective recapping of decapped $RNA1_{fs}$ by protein A could increase $RNA1_{fs}$ stability, we examined $RNA1_{fs}$ levels in wt and *xrn1*$^-$ mutant yeast. If protein A-stimulated $RNA1_{fs}$ accumulation was due only to $RNA1_{fs}$ recapping by protein A, thus inhibiting $RNA1_{fs}$ degradation, then protein A_{D692E} should have no effect on $RNA1_{fs}$ levels in *xrn1*$^-$ yeast. Furthermore, the equal $RNA1_{fs}$ levels in *xrn1*$^-$ yeast with or without protein A_{D692E} should match the high $RNA1_{fs}$ levels in wt yeast expressing protein A_{D692E}. Instead, we found that protein A still stimulated $RNA1_{fs}$ accumulation in *xrn1*$^-$ yeast approximately sixfold (Fig. 3, lanes 11 and 12). Additionally, $RNA1_{fs}$ levels in *xrn1*$^-$ yeast lacking protein A_{D692E} were approximately fourfold lower than $RNA1_{fs}$ levels in wt yeast expressing protein A_{D692E} (Fig. 3, lanes 6 and 11). Thus, a protein A function or functions other than $RNA1_{fs}$ recapping caused increased $RNA1_{fs}$ accumulation prior to negative-strand RNA synthesis.

Protein A selectively induces $RNA1_{fs}$ membrane association. FHV replicates in association with the outer mitochondrial membrane (45). Consequently, FHV genomic RNA must localize to the outer mitochondrial membrane before or during RNA synthesis. To test if protein A-stabilized $RNA1_{fs}$ was membrane associated, we used a Nycodenz gradient membrane flotation assay. As expected, 18S rRNA and the cytoplasmic yeast protein PGK were recovered only in the soluble, cytoplasmic fraction at the bottom of the gradient, while protein A and a yeast mitochondrial porin protein were present in the membrane-associated fraction at the top of the gradient, as seen by Northern and Western blotting (Fig. 4A). In the absence of protein A, ~80% of $RNA1_{fs}$ was present at the bottom of the gradient, while in the presence of pFA_{D692E}-YFP,

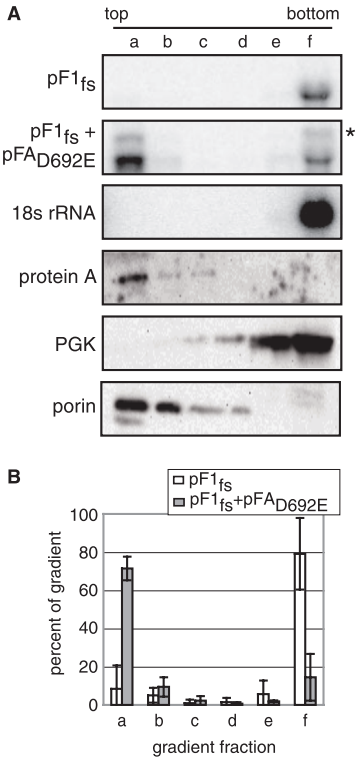

FIG. 4. Protein A induces RNA1 membrane association in yeast. Yeast cells transformed with $pF1_{fs}$ alone or together with pFA_{D692E}-YFP were grown in galactose medium to mid-log phase. Equal amounts of yeast were loaded under 5 to 35% discontinuous Nycodenz gradients and centrifuged for 4 to 5 hours at 40,000 rpm. Total RNA and protein were isolated from six equal-volume fractions from each gradient and analyzed by Northern blotting as described in the legend to Fig. 1 or by Western blotting with antibodies against protein A, PGK, and the yeast mitochondrial porin protein. The asterisk marks the protein A mRNA band (A). The amount of $RNA1_{fs}$ in each gradient fraction, determined from four independent experiments, was graphed as the percentage of $RNA1_{fs}$ in the entire gradient (B).

$RNA1_{fs}$ accumulation increased and ~70% of $RNA1_{fs}$ was present at the top of the gradient (Fig. 4A and B). As described for Fig. 2, in Fig. 4A the entire blot intensity for $pF1_{fs}$ alone was increased relative to that for the $pF1_{fs}$-plus-pF_{AD692E}-YFP blot to visualize the fraction f band. See Fig. 1B, lanes 3 and 5, for the actual relative band intensities of $RNA1_{fs}$ in the absence or presence of pFA_{D692E} under these conditions.

To determine if protein A preferentially increased the accumulation and membrane association of $RNA1_{fs}$ relative to those of nonviral RNAs, we used a cell fractionation assay. Centrifugation of a cell lysate created a membrane-enriched pellet(P) fraction and a membrane-depleted, cytoplasmic supernatant (S) fraction. Total RNA was isolated from the S and P fractions and an unfractionated yeast aliquot (total [T]). Equal fractions of yeast expressing no plasmids or the selectable plasmid $pF1_{fs}$, pGlobin, or pYFP in the presence or absence of pFA_{D692E} or pFA_{D692E}-YFP were analyzed by Northern blotting with ^{32}P-labeled RNA probes against positive-strand RNA1, selected cellular mRNAs, globin mRNA, or YFP mRNA. $pF1_{fs}$ alone yielded a very low level of $RNA1_{fs}$ accumulation that was mostly localized to the S fraction (Fig. 5A). However, when $pF1_{fs}$ and pFA_{D692E}-YFP were coex-

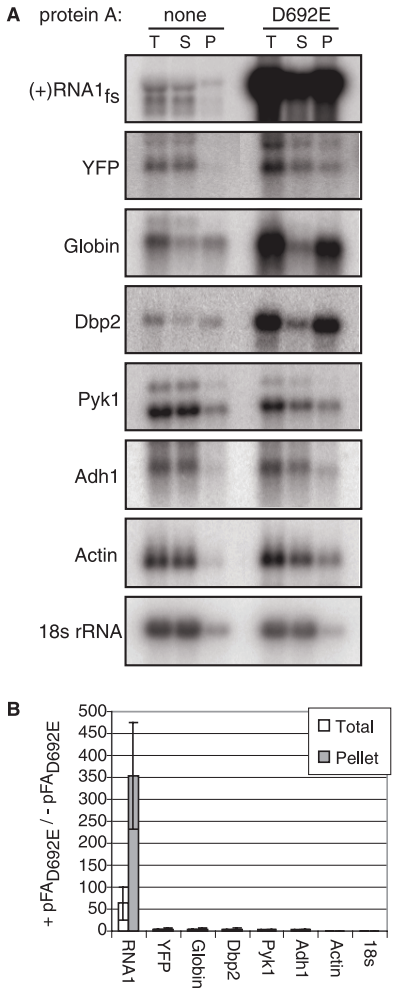

FIG. 5. Protein A selectively induces FHV $RNA1_{fs}$ membrane association. (A) Yeast cells expressing no plasmids or a selectable plasmid (pGlobin, pYFP, or $pF1_{fs}$) in the presence or absence of protein A_{D692E} were grown in galactose medium to mid-log phase and spheroplasted. Half of each sample was centrifuged for 5 minutes at 20,000 rpm to separate the membrane-enriched P fraction from the cytosolic S fraction, and half of each sample was untreated (T). Total RNA was isolated from each fraction, and equal amounts of RNA (2 μg of T) were analyzed by Northern blotting with [^{32}P]cRNA probes against positive-strand RNA1, globin mRNA, YFP mRNA, *DBP2* mRNA, *PYK1* mRNA, *ADH1* mRNA, *actin* mRNA, and 18S rRNA. (B) RNA levels in the T or P fractions in the presence and absence of pFA_{D692E}, determined from three independent experiments.

pressed, the $RNA1_{fs}$ pool in the S fraction was joined by a larger pool of $RNA1_{fs}$ in the P fraction (Fig. 5A). Protein A increased $RNA1_{fs}$ levels ~60-fold and ~350-fold in the T and P fractions, respectively (Fig. 5B). The level of protein A-stimulated total $RNA1_{fs}$ accumulation determined in this cell fractionation assay was higher than the 14-fold increase shown in Fig. 1. This difference was likely due to minor assay differences, such as the cell lysis and subsequent fractionation time prior to RNA extraction and necessary differences in the RNA extraction methods themselves (see Materials and Methods), and likely primarily reflected preferential decay of $RNA1_{fs}$ in the absence of protein A. Despite these differences, both assays show that protein A greatly increases $RNA1_{fs}$ accumulation. In contrast, protein A had no detectable effect on *PYK1* mRNA, *ADH1* mRNA, *actin* mRNA, and 18S rRNA (Fig. 5). Interestingly, protein A also increased the accumulation of globin mRNA, YFP mRNA, and *DBP2* mRNA (Fig. 5A). However, the effects of protein A on these cellular RNAs were dramatically less (2- to 4-fold and 3- to 5-fold increases in the T and P fractions, respectively) than the 60- to 350-fold increase for $RNA1_{fs}$ (Fig. 5A and B).

Protein A stimulates $RNA1_{fs}$ membrane association in *Drosophila melanogaster*. Since FHV naturally infects insects, we next analyzed the ability of protein A to stimulate membrane association in *Drosophila melanogaster* cells, which support productive FHV infection. To analyze $RNA1_{fs}$ levels in the absence and presence of protein A_{D692E} in *Drosophila* cells, we transfected these cells with plasmid $pIE1\text{-}F1_{fs}$ in the absence or presence of $pIE1\text{-}FA_{D692E}$, which expressed $RNA1_{fs}$ and protein A_{D692E}, respectively, from the baculovirus IE1 protein promoter. Two days after transfection, cells were harvested, lysed by Dounce homogenization, and assayed by flotation as described for Fig. 4. Since plasmid transfection levels in *D. melanogaster* cells are low and $RNA1_{fs}$ levels were further diluted by fractionation in flotation gradients, Northern blotting was insufficiently sensitive to reliably analyze $RNA1_{fs}$ levels in each gradient fraction. Accordingly, real-time RT-PCR was performed on DNase-treated RNA (5 ng) samples, using primer sets that selected for the wt FHV 5′ UTR of $RNA1_{fs}$, thus avoiding coamplification of protein A_{D692E} mRNA. In parallel, *Drosophila* actin mRNA was analyzed by RT-PCR to verify assay functionality and provide an internal control.

When $RNA1_{fs}$ was expressed alone in *D. melanogaster*, 16% and 56% of $RNA1_{fs}$ were present at the top and bottom of the gradient, respectively (Fig. 6A). However, when protein A_{D692E} was expressed with $RNA1_{fs}$ in *D. melanogaster*, the distribution reversed, with 62% and 20% of $RNA1_{fs}$ present at the top and bottom of the gradient, respectively (Fig. 6A). As expected, Western blotting showed that protein A and the voltage-dependent anion-channel mitochondrial porin protein localized to the top of the gradient, while actin protein was found at the bottom (data not shown). Thus, the behavior of $RNA1_{fs}$ and the effect of protein A_{D692E} on $RNA1_{fs}$ association with membranes were equivalent in *Drosophila* cells (Fig. 6A) and yeast (Fig. 4). In contrast, the presence of protein A_{D692E} did not increase total $RNA1_{fs}$ levels in *Drosophila* cells, as determined by Northern blotting and quantitative real-time RT-PCR (Fig. 6B). This result differs from the 14-fold protein A-stimulated $RNA1_{fs}$ accumulation effect seen in yeast (Fig. 1).

Conceivably, this difference in protein A-mediated $RNA1_{fs}$ accumulation in yeast and *Drosophila* cells might result from greater protein A expression in yeast than that in *Drosophila*. Therefore, we determined the ratio of protein A to $RNA1_{fs}$ in both yeast and *Drosophila* cells expressing $RNA1_{fs}$ and protein A_{D692E} (Fig. 6C). Protein A levels and total RNA (75 ng) were analyzed by Western blotting and real-time RT-PCR, respectively, as shown in Fig. 1 and described above. Total protein levels were determined using a modified Bradford assay that was compatible with reducing agents. The assays revealed that there were no significant differences between yeast and *Drosophila* cells in the ratios of protein A to total protein, $RNA1_{fs}$ to total RNA, and thus, protein A to $RNA1_{fs}$ (Fig. 6C). Con-

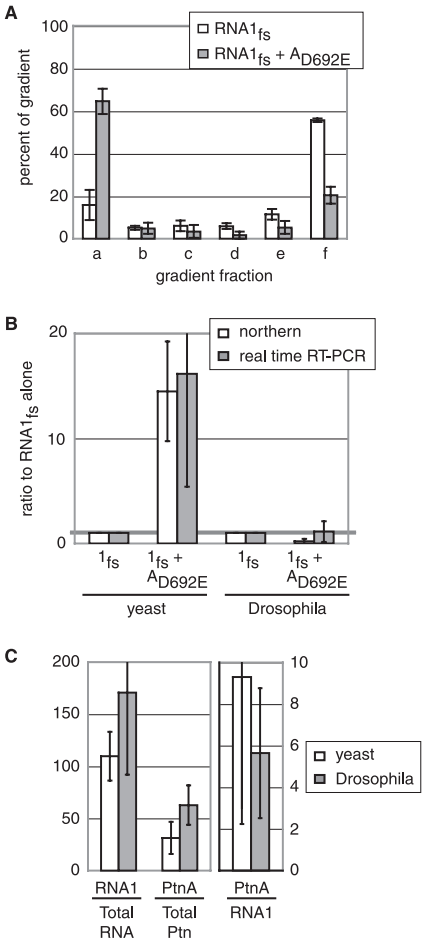

FIG. 6. Protein A induces $RNA1_{fs}$ membrane association in *Drosophila*. *D. melanogaster* cells expressing $RNA1_{fs}$ alone or together with protein A_{D692E} were collected 2 days after transfection. (A) Flotation and RNA extraction were done as described in the legend to Fig. 4. One-step real-time RT-PCR was performed on 5 ng of RNA, using primers and a probe specific for either RNA1 or *actin* mRNA. The $RNA1_{fs}$ amount in each gradient fraction, determined from four independent experiments, was graphed as the percentage of $RNA1_{fs}$ in the entire gradient. (B) Total RNA was extracted and analyzed by Northern blotting as described in the legend to Fig. 1 or by real-time RT-PCR as described above. Data from at least three independent experiments are shown. (C) Protein and RNA were extracted from equal cell volumes of yeast or *Drosophila* expressing $RNA1_{fs}$ and protein A_{D692E} and were analyzed by Western blotting for protein A as described in the legend to Fig. 1 and by real-time RT-PCR for positive-strand RNA1 as described above, except that 75 ng of total RNA was used. The ratios of protein A Boehringer light units to μg of total protein (Ptn A/total Ptn), positive-strand RNA1 molecules per ng of RNA loaded to ng of total RNA (RNA1/total RNA), and protein A/total protein to RNA1/total RNA (Ptn A/RNA1) are graphed on two different scales. Averages from three independent experiments are shown.

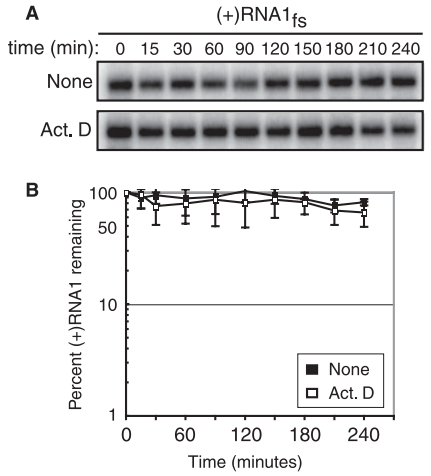

FIG. 7. $RNA1_{fs}$ is stable in *Drosophila* cells. *D. melanogaster* cells expressing $RNA1_{fs}$ alone were treated with actinomycin D or dimethyl sulfoxide (None) 2 days after transfection. (A) Total RNA was extracted from equal cell aliquots collected 0 to 4 hours after treatment and analyzed by Northern blotting as described in the legend to Fig. 1 (except that 4 μg of RNA was used). (B) RNA levels determined from three independent experiments were graphed as the percentage of positive-strand $RNA1_{fs}$ remaining compared to that at time zero, using the same scale as that in Fig. 2B.

sequently, differences in protein A expression levels did not explain the differences in protein A-mediated $RNA1_{fs}$ accumulation in yeast and *Drosophila* cells.

Differences in $RNA1_{fs}$ stability in the absence of protein A could also affect protein A-mediated $RNA1_{fs}$ accumulation levels. In these experiments with *Drosophila* cells, cellular transcription of plasmid pIE1-$F1_{fs}$ was the only source of $RNA1_{fs}$. Consequently, to measure $RNA1_{fs}$ stability, we treated *Drosophila* cells with actinomycin D at 20 μg/ml 2 days after transfection with pIE1-$F1_{fs}$ to inhibit cellular transcription. Cells were collected at 10 time points over a 4-hour time period after actinomycin D treatment, and total RNA (4 μg) was isolated and analyzed by Northern blotting. Cellular transcription was inhibited within 30 min of actinomycin D treatment, as seen by labeling with [^{32}P]UTP for 15 min prior to each time point (data not shown). However, even 4 hours after actinomycin D treatment, $RNA1_{fs}$ levels were indistinguishable from $RNA1_{fs}$ levels in untreated *Drosophila* cells (Fig. 7) or in *Drosophila* cells expressing protein A_{D692E}. Consequently, the half-life of $RNA1_{fs}$ in the absence of protein A in *Drosophila* cells was at least greater than 3 hours, and thus dramatically higher than the approximately 4-min half-life of $RNA1_{fs}$ in yeast (Fig. 2 and 7). Thus, differing $RNA1_{fs}$ intrinsic stabilities in yeast and *Drosophila* cells lacking protein A appear to account for the difference between the abilities of protein A_{D692E} to stimulate $RNA1_{fs}$ accumulation in yeast and *Drosophila* cells.

Protein A region(s) required for $RNA1_{fs}$ recruitment. Protein A is a multifunctional protein, and different regions of protein A are required for its many functions. A transmembrane domain and additional mitochondrial targeting signals are encompassed in the N-terminal 35 and 47 aa of protein A, respectively (44). Regions within and including aa 1 to 400 and 700 to 800 of protein A self-interact in vivo (15). In addition, the eight conserved RdRp motifs of protein A are located between aa 513 and 752 (35). We have shown here that another function of protein A is to recruit RNA1 to a membrane-associated state (Fig. 1 to 7). To determine the region(s) of protein A required for this new function, we made 29 in-frame deletion mutants that spanned the length of protein A (Fig. 8A and 9A). Yeast cells expressing $RNA1_{fs}$ and protein A_{D692E} deletion mutants were assayed for total $RNA1_{fs}$ accumulation

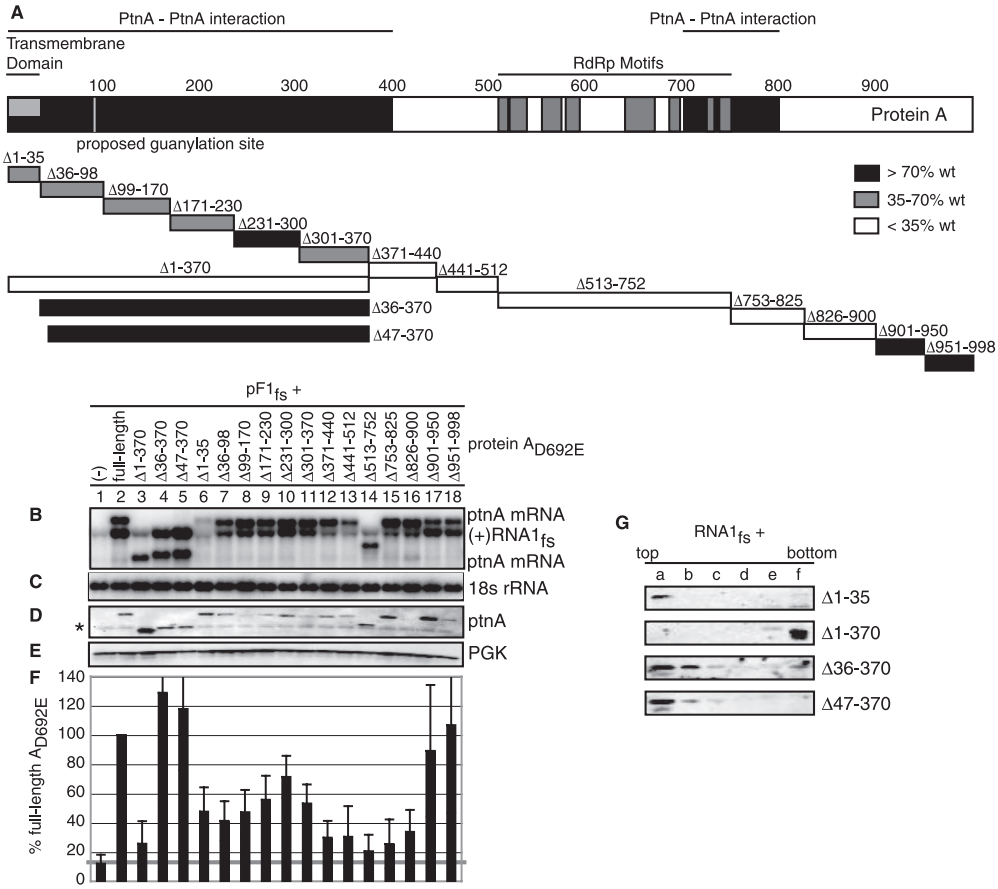

FIG. 8. Membrane association and the RdRp region of protein A are required for $RNA1_{fs}$ accumulation. (A) Protein A map which identifies the transmembrane domain, protein A self-interaction domains, and eight conserved RdRp motifs. Sixteen deletions within protein A_{D692E} were made and are indicated by boxes. Yeast cells were transformed with $pF1_{fs}$ alone or together with full-length or a deletion mutant of pFA_{D692E} or pFA_{D692E}-YFP. Total RNA and protein were extracted and analyzed as described in the legend to Fig. 1 for positive-strand $RNA1_{fs}$ (B), 18S rRNA (C), protein A (D), and PGK (E). The asterisk in panel D denotes a background band. Levels of $RNA1_{fs}$ accumulation, determined from at least four independent experiments after normalization to 18S rRNA, were expressed as percentages of $RNA1_{fs}$ accumulation in the presence of full-length pFA_{D692E}-YFP (F) and are indicated by deletion box shading (A).

and graphed as the percentage of $RNA1_{fs}$ accumulation when $RNA1_{fs}$ and full-length protein A_{D692E} were expressed (Fig. 8A and F). Although minor variations in accumulation of the various protein A derivatives occurred in some experiments (Fig. 8D and 9D), over many experiments the average levels of the various protein A deletion mutants and full-length protein A_{D692E} were similar. Consequently, any differences in average $RNA1_{fs}$ accumulation were due to differences in the specific activities, not expression, of each protein A deletion mutant.

Multiple results implied that membrane association of protein A was required for $RNA1_{fs}$ accumulation. Eliminating protein A membrane association by deleting the N-terminal 370 aa (Δ1-370) (Fig. 8A and G) reduced $RNA1_{fs}$ accumulation nearly fourfold (Fig. 8B, lane 3). Furthermore, adding back just 35 to 47 aa of protein A sequence sufficient for mitochondrial localization, including the transmembrane domain (aa 17 to 35), completely restored protein A membrane association and $RNA1_{fs}$ accumulation (Δ36-370 and Δ47-370) (Fig. 8B, lanes 4 and 5, and G) (44, 46). Despite occasional small fluctuations in individual $RNA1_{fs}$ accumulation measurements, deleting the protein A transmembrane domain (Δ1-35) caused a milder, on average approximately twofold decrease, in $RNA1_{fs}$ accumulation (Fig. 8B and F, lanes 6) but maintained protein A membrane association (Fig. 8G). Despite the fact that the entire region of aa 36 to 370 was dispensable for protein A-mediated $RNA1_{fs}$ accumulation (Δ36-370) (Fig. 8B, lane 4), various partial deletions of 60 to 70 aa between aa 35 and 370 of protein A also caused milder reductions in protein A-mediated $RNA1_{fs}$ accumulation (Δ36-98, Δ99-170, Δ171-230, Δ231-300, and Δ301-370) (Fig. 8B, lanes 7 to 11), suggesting a perturbation of protein folding, interaction, or similar functions.

The C-terminal 100 aa of protein A (Δ901-950 and Δ951-998) were also dispensable for protein A-stimulated $RNA1_{fs}$ accumulation (Fig. 8, lanes 17 and 18). In contrast, although protein A RdRp activity was not required for $RNA1_{fs}$ accumulation (Fig. 1), deletion of the RdRp region (Δ513-752) significantly reduced $RNA1_{fs}$ accumulation (Fig. 8B, lane 14, and 9B). To explore this further, we made separate deletions of each RdRp motif, which ranged in size from 9 to 35 aa, and the spaces between these motifs (Fig. 9A). The first RdRp motif (R1 [Δ513-752]) was dispensable for $RNA1_{fs}$ accumulation

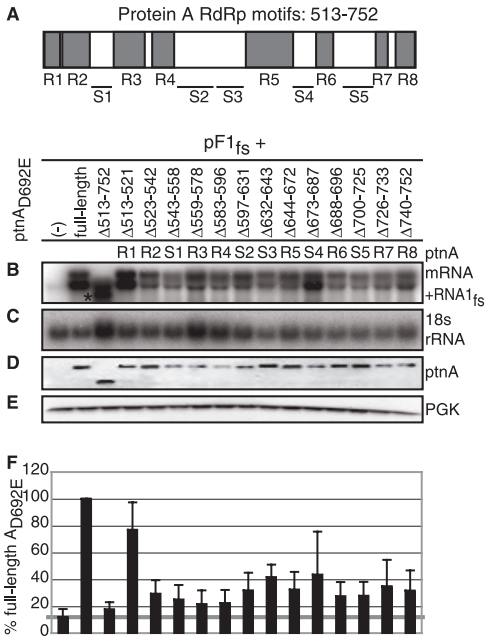

FIG. 9. $RNA1_{fs}$ accumulation requires many RdRp motifs. (A) Map of eight conserved RdRp motifs in protein A. Deletions of RdRp motifs are labeled R1 through R8. Deletions of spaces between RdRp motifs are labeled S1 through S5. Yeast cells were transformed with $pF1_{fs}$ alone or together with full-length or deletion mutant pFA_{D692E}-YFP. The asterisk in panel B denotes a protein A mRNA band. Total RNAs and proteins were extracted and analyzed as described in the legend to Fig. 7 (B to F). Averages from six independent experiments are shown.

(Fig. 9B, lane R1). In contrast, deletion of all other RdRp motifs and spaces between RdRp motifs reduced $RNA1_{fs}$ accumulation to approximately threefold lower than $RNA1_{fs}$ levels expressed in the presence of full-length protein A_{D692E}-YFP, although deletions of the third and fourth spaces between RdRp motifs were the least defective (Fig. 9). $RNA1_{fs}$ accumulation also required protein A regions immediately surrounding the RdRp motifs, since deletions of approximately 70 aa on either side of the RdRp motifs (Δ371-440, Δ441-512, Δ753-825, and Δ826-900) significantly reduced $RNA1_{fs}$ accumulation (Fig. 8B, lanes 12, 13, 15, and 16).

These results show that efficient protein A-mediated RNA1 recruitment requires protein A membrane association and the regions surrounding and including RdRp motifs. However, with the exception of the transmembrane domain, the N-terminal 370 aa of protein A, including some protein A self-interaction domains, and the C-terminal 100 aa of protein A are dispensable for protein A-mediated RNA1 recruitment.

DISCUSSION

In this study, we used FHV to analyze selected aspects of positive-strand RNA virus replication, revealing a new function for FHV protein A in recruiting genomic RNA1 to a membrane-associated state. As discussed below, our results imply that during an early stage of replication prior to negative-strand RNA synthesis, multiple regions of protein A, including regions required for other protein A functions, act together to recruit RNA1 to membranes for FHV RNA replication complex formation.

Protein A recruits RNA1 to a membrane-associated state. In both *Drosophila* and yeast cells, FHV protein A induced otherwise cytoplasmic RNA1 to become largely membrane associated, causing similar near-inversions of the distribution of RNA1 between soluble and membrane-associated fractions in both cell types (Fig. 4 and 6). This strong membrane localization was induced by protein A even when viral RNA synthesis was blocked by an RdRp active site mutation and was strongly selective for FHV RNA, increasing the accumulation of $RNA1_{fs}$ in the membrane-associated pellet fraction 70- to >300-fold more than that of diverse nonviral mRNAs (Fig. 5). Since protein A is the sole FHV protein required for RNA replication and is a transmembrane protein localized almost exclusively to outer mitochondrial membranes, the results imply that protein A recruits RNA1 prior to RNA replication to the outer mitochondrial membranes, where FHV RNA replication complexes form (44, 45).

However, in yeast, this protein A-induced membrane association was linked with a >10-fold increase in RNA1 accumulation, while in *Drosophila* cells no significant increase in RNA1 accumulation occurred (Fig. 1 and 6B). This difference in protein A-mediated RNA1 accumulation was not caused by differences in the amount of protein A available in each cell type to confer RNA1 stability, since the ratios of protein A to RNA1 in yeast and *Drosophila* cells were similar (Fig. 6C). Rather, in yeast cells, which are widely diverged from FHV's natural insect host cells, the >10-fold increase reflected the fact that RNA1 was stable in the presence of protein A (>60-min half-life) but had low basal stability and accumulation in the absence of protein A (4-min half-life) (Fig. 2). In contrast, in *Drosophila* cells, which support productive FHV infection (8, 63), the intrinsic stability (>3-hour half-life) of RNA1 was much higher than that in yeast (Fig. 7). Accordingly, the accumulation of RNA1 without protein A was close to that with protein A (Fig. 6B). Similarly, the BMV 1a protein, which recruits viral RNA replication templates to a membrane-associated, highly stable state for RNA replication, increased BMV genomic RNA3 stability and accumulation ~10-fold in yeast, but little or not at all in *Nicotiana benthamiana* cells, apparently because the basal stability of plant-adapted BMV RNA in the absence of 1a is much higher in plant cells than in yeast cells (25, 32, 66).

Nevertheless, the short, ~5-min half-life of BMV and FHV RNAs in yeast cells in the absence of viral factors has been useful as a marker to reveal and follow the 1a- and protein A-induced changes in the state of viral RNA. For BMV, multiple additional studies have revealed that the 1a-induced increase in viral RNA stability reflects important effects associated with recruitment to a membrane-associated state, including translation inhibition and sequestration of the RNA in a nuclease-resistant compartment (1, 32, 62, 68). Since BMV and FHV replicate their RNAs in similar, virus-induced membrane invaginations (45, 62), similar effects appear likely to underlie the related protein A-induced changes in the state of FHV RNA1. The increase in RNA1 stability, and thus accumulation, was not significantly due to the predicted ability of protein A to cap FHV RNAs (33), since protein A increased $RNA1_{fs}$ accumulation sixfold even in yeast lacking the Xrn1p

5′-to-3′ exonuclease that degrades uncapped RNAs (Fig. 3) (37, 65, 67). A lack of RNA1 recapping by protein A is consistent with the fact that cellular decapping enzymes produce 5′-monophosphate ends (67), while known positive-strand RNA virus capping pathways require 5′-diphosphate substrates (2, 3, 14, 30, 41), and with continuing stimulation of RNA1 accumulation after deleting the predicted guanylyltransferase active site (aa 91 to 93) from protein A (Δ36-370 and Δ47-370) (Fig. 8, lanes 4 and 5) (33).

Protein A regions required for RNA1 recruitment. Protein A was the only viral protein required for FHV genomic RNA1 recruitment to membranes, implying that protein A interacts directly or indirectly (via host proteins) with FHV RNA1 to recruit it to a membrane-associated state. Recruiting FHV genomic RNAs required both membrane-targeting domains and the RdRp domain of protein A (Fig. 8 and 9). This association of RNA recruitment with the FHV RdRp domain differs from the case for BMV, cucumber necrosis tombusvirus, and tomato bushy stunt tombusvirus, for which genomic RNA recruitment to membranes requires only viral protein 1a or p33, respectively, which contain membrane-targeting and other domains but lack the RdRp domains carried by other proteins of these viruses (47, 51, 54, 55, 62). Use of the FHV protein A RdRp domain for template recruitment as well as polymerization may reflect appropriate or essential economy for a virus with a single RNA replication protein. Moreover, like the case for FHV, carnation Italian ringspot tombusvirus recruitment of DI-RNAs to a stabilized state is significantly enhanced by the presence of both membrane-targeting and RdRp domains, carried by the viral p36 and p95 proteins, respectively, although either p36 or p95 confers some DI-RNA stabilization (35, 49, 56, 57). Additionally, the poliovirus protein 3CD, containing protease and RdRp domains, is required to bind a 5′ cloverleaf in poliovirus RNA to mediate the switch from translation to viral RNA replication, a step that is at least a precursor to recruiting viral RNA to the replication complex (24). When expressed in vitro, 3CD and 3C, but not 3D, can bind the 5′ cloverleaf (70). However, mutations in both the 3C and 3D regions of 3CD rescue complementary changes in the 5′-cloverleaf structure, suggesting that regions in both proteins are important for RNA binding (69).

While active site mutation showed that polymerase activity was not required, nearly all deletions within or flanking the conserved RdRp motifs of FHV protein A dramatically suppressed protein A-stimulated RNA1 accumulation (Fig. 8 and 9). The strong effect of even small deletions in this region suggests that proper folding of the RdRp domain may be important for RNA1 recruitment. Such folding might be required whether the RdRp domain contributes to recruitment by RNA or to protein interactions that are the same or distinct from those in RNA polymerization. For example, multiple regions surrounding and including the conserved RdRp motifs of foot-and-mouth disease virus 3D polymerase are involved in binding RNA templates, as seen by X-ray crystallography (19), and tomato bushy stunt virus p92 contains multiple RNA binding sites flanking and overlapping its conserved RdRp motifs (54).

Our deletion analysis revealed a parallel between the membrane association of protein A derivatives and their ability to stimulate $RNA1_{fs}$ accumulation. Deleting the N-terminal 370 aa of protein A (Δ1-370) eliminated protein A-membrane association and increased $RNA1_{fs}$ recruitment, while retaining protein A sequences sufficient for membrane association and mitochondrial targeting (Δ36-370 and Δ47-370) fully restored protein A stimulation of $RNA1_{fs}$ accumulation (Fig. 8). Deleting the transmembrane domain (Δ1-35) significantly inhibited but did not completely eliminate increased $RNA1_{fs}$ accumulation (Fig. 8). However, this derivative remained largely membrane associated (Fig. 8) (46), showing that protein A has more than one mode of membrane association and explaining the remaining RNA1 recruitment activity without violating the membrane association correlation.

Several functions may contribute to the link between protein A-membrane association and increased RNA1 stability/accumulation in yeast. Membrane association might alter the protein A conformation and would increase the local protein A concentration, promoting protein A multimerization and potentially cooperative binding to RNA1. Protein A forms multimers in vivo, and this ability is linked to successful RNA replication (15). While some N-proximal protein A self-interaction domains were dispensable for increased RNA1 accumulation, a self-interaction domain overlapping the RdRp region was required and might represent a significant contribution of the RdRp domain (Fig. 8) (15). Similarly, self-interaction of tomato bushy stunt virus p33 is required for DI-RNA recruitment to the membrane sites of replication complex formation (47, 51). As found for BMV (62), protein A-membrane binding and the FHV-specific outer mitochondrial membrane invaginations associated with RNA replication (45) may be important for compartmentalizing RNA1 away from cellular translation and RNA decay pathways. We also cannot rule out that membrane association may be important for protein A or RNA1 association with host factors.

The results reported here for FHV in both *D. melanogaster* cells and *S. cerevisiae* cells show some strong parallels with BMV and with recent emerging results for tombusviruses. In all cases, a viral replication protein recruits genomic RNA to membranes prior to negative-strand RNA synthesis (1, 47, 51, 62). Such recruitment is often accompanied by an increase in genomic RNA stability and accumulation that is tightly linked to RNA membrane association (12, 32, 62, 66). Membrane-targeting domains and, in some cases, RdRp domains and self-interaction domains within the viral replication proteins are required for these effects on genomic RNA (12, 47, 49, 51, 54, 66). Given the many other substantial differences between FHV, BMV, and the tombusviruses, these related features suggest that some of the major principles involved in the RNA recruitment processes revealed here may be applicable to a range of positive-strand RNA viruses.

ACKNOWLEDGMENTS

We thank Paul Friesen, Ben Kopek, and Billy Dye for helpful comments and David Miller, David Kushner, Billy Dye, Erik Settles, and Paul Friesen for various plasmids.

This work was supported by NIH grant GM35072. P.A. is an investigator of the Howard Hughes Medical Institute. P.M.V. gratefully acknowledges support from a Howard Hughes Medical Institute predoctoral fellowship and an NIH Predoctoral Training grant in Molecular Biosciences (T32 GM07215).

REFERENCES

1. **Ahlquist, P.** 2006. Parallels among positive-strand RNA viruses, reverse-transcribing viruses and double-stranded RNA viruses. Nat. Rev. Microbiol. **4:**371–382.
2. **Ahola, T., and P. Ahlquist.** 1999. Putative RNA capping activities encoded by brome mosaic virus: methylation and covalent binding of guanylate by replicase protein 1a. J. Virol. **73:**10061–10069.
3. **Ahola, T., and L. Kaariainen.** 1995. Reaction in alphavirus mRNA capping: formation of a covalent complex of nonstructural protein nsP1 with 7-methyl-GMP. Proc. Natl. Acad. Sci. USA **92:**507–511.
4. **Argos, P.** 1988. A sequence motif in many polymerases. Nucleic Acids Res. **16:**9909–9916.
5. **Ausubel, F. M., R. Brent, R. E. Kingston, D. D. Moore, J. G. Seidman, J. A. Smith, and K. Struhl (ed.).** 1987. Current protocols in molecular biology. John Wiley & Sons, Inc., New York, NY.
6. **Ball, L. A.** 1992. Cellular expression of a functional nodavirus RNA replicon from vaccinia virus vectors. J. Virol. **66:**2335–2345.
7. **Ball, L. A.** 1995. Requirements for the self-directed replication of flock house virus RNA 1. J. Virol. **69:**720–727.
8. **Ball, L. A., and K. L. Johnson.** 1998. Nodaviruses of insects, p. 225–267. *In* L. K. Miller and L. A. Ball (ed.), The insect viruses. Plenum Publishing Corporation, New York, NY.
9. **Benzaghou, I., I. Bougie, and M. Bisaillon.** 2004. Effect of metal ion binding on the structural stability of the hepatitis C virus RNA polymerase. J. Biol. Chem. **279:**49755–49761.
10. **Cartier, J. L., P. A. Hershberger, and P. D. Friesen.** 1994. Suppression of apoptosis in insect cells stably transfected with baculovirus p35: dominant interference by N-terminal sequences p35(1-76). J. Virol. **68:**7728–7737.
11. **Chen, J., and P. Ahlquist.** 2000. Brome mosaic virus polymerase-like protein 2a is directed to the endoplasmic reticulum by helicase-like viral protein 1a. J. Virol. **74:**4310–4318.
12. **Chen, J., A. Noueiry, and P. Ahlquist.** 2001. Brome mosaic virus protein 1a recruits viral RNA2 to RNA replication through a 5′-proximal RNA2 signal. J. Virol. **75:**3207–3219.
13. **Dasgupta, R., A. Ghosh, B. Dasmahapatra, L. A. Guarino, and P. Kaesberg.** 1984. Primary and secondary structure of black beetle virus RNA2, the genomic messenger for BBV coat protein precursor. Nucleic Acids Res. **12:**7215–7223.
14. **Dunigan, D. D., and M. Zaitlin.** 1990. Capping of tobacco mosaic virus RNA. Analysis of viral-coded guanylyltransferase-like activity. J. Biol. Chem. **265:** 7779–7786.
15. **Dye, B. T., D. J. Miller, and P. Ahlquist.** 2005. In vivo self-interaction of nodavirus RNA replicase protein A revealed by fluorescence resonance energy transfer. J. Virol. **79:**8909–8919.
16. **Egger, D., and K. Bienz.** 2005. Intracellular location and translocation of silent and active poliovirus replication complexes. J. Gen. Virol. **86:**707–718.
17. **Egger, D., B. Wolk, R. Gosert, L. Bianchi, H. E. Blum, D. Moradpour, and K. Bienz.** 2002. Expression of hepatitis C virus proteins induces distinct membrane alterations including a candidate viral replication complex. J. Virol. **76:**5974–5984.
18. **Elazar, M., P. Liu, C. M. Rice, and J. S. Glenn.** 2004. An N-terminal amphipathic helix in hepatitis C virus (HCV) NS4B mediates membrane association, correct localization of replication complex proteins, and HCV RNA replication. J. Virol. **78:**11393–11400.
19. **Ferrer-Orta, C., A. Arias, R. Perez-Luque, C. Escarmis, E. Domingo, and N. Verdaguer.** 2004. Structure of foot-and-mouth disease virus RNA-dependent RNA polymerase and its complex with a template-primer RNA. J. Biol. Chem. **279:**47212–47221.
20. **Friesen, P. D., and R. R. Rueckert.** 1982. Black beetle virus: messenger for protein B is a subgenomic viral RNA. J. Virol. **42:**986–995.
21. **Friesen, P. D., and R. R. Rueckert.** 1981. Synthesis of black beetle virus proteins in cultured *Drosophila* cells: differential expression of RNAs 1 and 2. J. Virol. **37:**876–886.
22. **Gallagher, T. M., P. D. Friesen, and R. R. Rueckert.** 1983. Autonomous replication and expression of RNA 1 from black beetle virus. J. Virol. **46:**481–489.
23. **Gallagher, T. M., and R. R. Rueckert.** 1988. Assembly-dependent maturation cleavage in provirions of a small icosahedral insect ribovirus. J. Virol. **62:** 3399–3406.
24. **Gamarnik, A. V., and R. Andino.** 1998. Switch from translation to RNA replication in a positive-stranded RNA virus. Genes Dev. **12:**2293–2304.
25. **Gopinath, K., B. Dragnea, and C. Kao.** 2005. Interaction between brome mosaic virus proteins and RNAs: effects on RNA replication, protein expression, and RNA stability. J. Virol. **79:**14222–14234.
26. **Gosert, R., D. Egger, V. Lohmann, R. Bartenschlager, H. E. Blum, K. Bienz, and D. Moradpour.** 2003. Identification of the hepatitis C virus RNA replication complex in Huh-7 cells harboring subgenomic replicons. J. Virol. **77:**5487–5492.
27. **Guarino, L. A., A. Ghosh, B. Dasmahapatra, R. Dasgupta, and P. Kaesberg.** 1984. Sequence of the black beetle virus subgenomic RNA and its location in the viral genome. Virology **139:**199–203.
28. **Heinlein, M., H. S. Padgett, J. S. Gens, B. G. Pickard, S. J. Casper, B. L. Epel, and R. N. Beachy.** 1998. Changing patterns of localization of the tobacco mosaic virus movement protein and replicase to the endoplasmic reticulum and microtubules during infection. Plant Cell **10:**1107–1120.
29. **Herrick, D., R. Parker, and A. Jacobson.** 1990. Identification and comparison of stable and unstable mRNAs in *Saccharomyces cerevisiae*. Mol. Cell. Biol. **10:**2269–2284.
30. **Huang, Y. L., Y. H. Hsu, Y. T. Han, and M. Meng.** 2005. mRNA guanylation catalyzed by the *S*-adenosylmethionine-dependent guanylyltransferase of bamboo mosaic virus. J. Biol. Chem. **280:**13153–13162.
31. **Jablonski, S. A., and C. D. Morrow.** 1995. Mutation of the aspartic acid residues of the GDD sequence motif of poliovirus RNA-dependent RNA polymerase results in enzymes with altered metal ion requirements for activity. J. Virol. **69:**1532–1539.
32. **Janda, M., and P. Ahlquist.** 1998. Brome mosaic virus RNA replication protein 1a dramatically increases in vivo stability but not translation of viral genomic RNA3. Proc. Natl. Acad. Sci. USA **95:**2227–2232.
33. **Johnson, K. N., K. L. Johnson, R. Dasgupta, T. Gratsch, and L. A. Ball.** 2001. Comparisons among the larger genome segments of six nodaviruses and their encoded RNA replicases. J. Gen. Virol. **82:**1855–1866.
34. **Kamer, G., and P. Argos.** 1984. Primary structural comparison of RNA-dependent polymerases from plant, animal and bacterial viruses. Nucleic Acids Res. **12:**7269–7282.
35. **Koonin, E. V.** 1991. The phylogeny of RNA-dependent RNA polymerases of positive-strand RNA viruses. J. Gen. Virol. **72:**2197–2206.
36. **Kujala, P., A. Ikaheimonen, N. Ehsani, H. Vihinen, P. Auvinen, and L. Kaariainen.** 2001. Biogenesis of the Semliki Forest virus RNA replication complex. J. Virol. **75:**3873–3884.
37. **Larimer, F. W., C. L. Hsu, M. K. Maupin, and A. Stevens.** 1992. Characterization of the XRN1 gene encoding a 5′→3′ exoribonuclease: sequence data and analysis of disparate protein and mRNA levels of gene-disrupted yeast cells. Gene **120:**51–57.
38. **Li, H., W. X. Li, and S. W. Ding.** 2002. Induction and suppression of RNA silencing by an animal virus. Science **296:**1319–1321.
39. **Lindenbach, B. D., J. Y. Sgro, and P. Ahlquist.** 2002. Long-distance base pairing in flock house virus RNA1 regulates subgenomic RNA3 synthesis and RNA2 replication. J. Virol. **76:**3905–3919.
40. **Lu, R., M. Maduro, F. Li, H. W. Li, G. Broitman-Maduro, W. X. Li, and S. W. Ding.** 2005. Animal virus replication and RNAi-mediated antiviral silencing in Caenorhabditis elegans. Nature **436:**1040–1043.
41. **Magden, J., N. Takeda, T. Li, P. Auvinen, T. Ahola, T. Miyamura, A. Merits, and L. Kaariainen.** 2001. Virus-specific mRNA capping enzyme encoded by hepatitis E virus. J. Virol. **75:**6249–6255.
42. **Magliano, D., J. A. Marshall, D. S. Bowden, N. Vardaxis, J. Meanger, and J. Y. Lee.** 1998. Rubella virus replication complexes are virus-modified lysosomes. Virology **240:**57–63.
43. **Mas, P., and R. N. Beachy.** 1999. Replication of tobacco mosaic virus on endoplasmic reticulum and role of the cytoskeleton and virus movement protein in intracellular distribution of viral RNA. J. Cell Biol. **147:**945–958.
44. **Miller, D. J., and P. Ahlquist.** 2002. Flock house virus RNA polymerase is a transmembrane protein with amino-terminal sequences sufficient for mitochondrial localization and membrane insertion. J. Virol. **76:**9856–9867.
45. **Miller, D. J., M. D. Schwartz, and P. Ahlquist.** 2001. Flock house virus RNA replicates on outer mitochondrial membranes in *Drosophila* cells. J. Virol. **75:**11664–11676.
46. **Miller, D. J., M. D. Schwartz, B. T. Dye, and P. Ahlquist.** 2003. Engineered retargeting of viral RNA replication complexes to an alternative intracellular membrane. J. Virol. **77:**12193–12202.
47. **Panavas, T., C. M. Hawkins, Z. Panaviene, and P. D. Nagy.** 2005. The role of the p33:p33/p92 interaction domain in RNA replication and intracellular localization of p33 and p92 proteins of cucumber necrosis tombusvirus. Virology **338:**81–95.
48. **Panaviene, Z., T. Panavas, and P. D. Nagy.** 2005. Role of an internal and two 3′-terminal RNA elements in assembly of tombusvirus replicase. J. Virol. **79:**10608–10618.
49. **Pantaleo, V., L. Rubino, and M. Russo.** 2004. The p36 and p95 replicase proteins of carnation Italian ringspot virus cooperate in stabilizing defective interfering RNA. J. Gen. Virol. **85:**2429–2433.
50. **Perrigoue, J. G., J. A. den Boon, A. Friedl, M. A. Newton, P. Ahlquist, and B. Sugden.** 2005. Lack of association between EBV and breast carcinoma. Cancer Epidemiol. Biomarkers Prev. **14:**809–814.
51. **Pogany, J., K. A. White, and P. D. Nagy.** 2005. Specific binding of tombusvirus replication protein p33 to an internal replication element in the viral RNA is essential for replication. J. Virol. **79:**4859–4869.
52. **Price, B. D., R. R. Rueckert, and P. Ahlquist.** 1996. Complete replication of an animal virus and maintenance of expression vectors derived from it in *Saccharomyces cerevisiae*. Proc. Natl. Acad. Sci. USA **93:**9465–9470.
53. **Price, B. D., M. Roeder, and P. Ahlquist.** 2000. DNA-directed expression of functional flock house virus RNA1 derivatives in *Saccharomyces cerevisiae*, heterologous gene expression, and selective effects on subgenomic mRNA synthesis. J. Virol. **74:**11724–11733.
54. **Rajendran, K. S., and P. D. Nagy.** 2003. Characterization of the RNA-

binding domains in the replicase proteins of tomato bushy stunt virus. J. Virol. **77:**9244–9258.
55. **Restrepo-Hartwig, M. A., and P. Ahlquist.** 1996. Brome mosaic virus helicase- and polymerase-like proteins colocalize on the endoplasmic reticulum at sites of viral RNA synthesis. J. Virol. **70:**8908–8916.
56. **Rubino, L., and M. Russo.** 1998. Membrane targeting sequences in tombusvirus infections. Virology **252:**431–437.
57. **Rubino, L., F. Weber-Lotfi, A. Dietrich, C. Stussi-Garaud, and M. Russo.** 2001. The open reading frame 1-encoded ('36K') protein of carnation Italian ringspot virus localizes to mitochondria. J. Gen. Virol. **82:**29–34.
58. **Salonen, A., T. Ahola, and L. Kaariainen.** 2005. Viral RNA replication in association with cellular membranes. Curr. Top. Microbiol. Immunol. **285:** 139–173.
59. **Sambrook, J., and D. Russell.** 2001. Molecular cloning: a laboratory manual, 3rd ed. Cold Spring Harbor Laboratory Press, Cold Spring Harbor, NY.
60. **Schlegel, A., T. H. Giddings, Jr., M. S. Ladinsky, and K. Kirkegaard.** 1996. Cellular origin and ultrastructure of membranes induced during poliovirus infection. J. Virol. **70:**6576–6588.
61. **Schneemann, A., V. Reddy, and J. E. Johnson.** 1998. The structure and function of nodavirus particles: a paradigm for understanding chemical biology. Adv. Virus Res. **50:**381–446.
62. **Schwartz, M., J. Chen, M. Janda, M. Sullivan, J. den Boon, and P. Ahlquist.** 2002. A positive-strand RNA virus replication complex parallels form and function of retrovirus capsids. Mol. Cell **9:**505–514.
63. **Scotti, P. D., S. Dearing, and D. W. Mossop.** 1983. Flock house virus: a nodavirus isolated from Costelytra zealandica (White) (Coleoptera: Scarabaeidae). Arch. Virol. **75:**181–189.
64. **Selling, B. H., R. F. Allison, and P. Kaesberg.** 1990. Genomic RNA of an insect virus directs synthesis of infectious virions in plants. Proc. Natl. Acad. Sci. USA **87:**434–438.
65. **Stevens, A.** 1980. Purification and characterization of a Saccharomyces cerevisiae exoribonuclease which yields 5′-mononucleotides by a 5′ leads to 3′ mode of hydrolysis. J. Biol. Chem. **255:**3080–3085.
66. **Sullivan, M. L., and P. Ahlquist.** 1999. A brome mosaic virus intergenic RNA3 replication signal functions with viral replication protein 1a to dramatically stabilize RNA in vivo. J. Virol. **73:**2622–2632.
67. **Tucker, M., and R. Parker.** 2000. Mechanisms and control of mRNA decapping in Saccharomyces cerevisiae. Annu. Rev. Biochem. **69:**571–595.
68. **Wang, X., W. M. Lee, T. Watanabe, M. Schwartz, M. Janda, and P. Ahlquist.** 2005. Brome mosaic virus 1a nucleoside triphosphatase/helicase domain plays crucial roles in recruiting RNA replication templates. J. Virol. **79:** 13747–13758.
69. **Yang, Y., R. Rijnbrand, S. Watowich, and S. M. Lemon.** 2004. Genetic evidence for an interaction between a picornaviral cis-acting RNA replication element and 3CD protein. J. Biol. Chem. **279:**12659–12667.
70. **Yin, J., A. V. Paul, E. Wimmer, and E. Rieder.** 2003. Functional dissection of a poliovirus *cis*-acting replication element [PV-cre(2C)]: analysis of single- and dual-cre viral genomes and proteins that bind specifically to PV-cre RNA. J. Virol. **77:**5152–5166.